Kinoshita, M., Tobin, H., Ashi, J., Kimura, G., Lallemant, S., Screaton, E.J., Curewitz, D., Masago, H., Moe, K.T., and the Expedition 314/315/316 Scientists
Proceedings of the Integrated Ocean Drilling Program, Volume 314/315/316

Data report: distribution of iodine concentration and ^{129}I in interstitial fluid in the Nankai Trough accretionary prism collected during IODP Expeditions 315 and 316[1]

Hitoshi Tomaru[2] and Udo Fehn[3]

Chapter contents

[1]Tomaru, H., and Fehn, U., 2012. Data report: distribution of iodine concentration and ^{129}I in interstitial fluid in the Nankai Trough accretionary prism collected during IODP Expeditions 315 and 316. *In* Kinoshita, M., Tobin, H., Ashi, J., Kimura, G., Lallemant, S., Screaton, E.J., Curewitz, D., Masago, H., Moe, K.T., and the Expedition 314/315/316 Scientists, *Proc. IODP,* 314/315/316: Washington, DC (Integrated Ocean Drilling Program Management International, Inc.). doi:10.2204/iodp.proc.314315316.220.2012
[2]Department of Earth and Planetary Science, University of Tokyo, Tokyo 113-0033, Japan. Correspondence author: tomaru@eps.s.u-tokyo.ac.jp
[3]Department of Earth and Environmental Sciences, University of Rochester, Rochester NY 14627, USA.

Abstract

Iodine concentration and $^{129}I/I$ ratios were determined in interstitial fluid collected from the Nankai Trough accretionary prism during Integrated Ocean Drilling Program (IODP) Expeditions 315 and 316. Iodine concentrations increase rapidly in the uppermost 100 m below the seafloor, before concentrations reach stable values between 200 and 400 µM, reflecting the advection of iodine released during the degradation of organic matter in deep sediments. The $^{129}I/I$ ratios in the interstitial fluid start just below preanthropogenic seawater values and decrease rapidly with depth to ratios ~400×10^{-15}. These ratios result in ages for the potential iodine source formation between 30 and 40 Ma, which are clearly older than the host sediments and demonstrate that advection of fluids is responsible for the observed distribution of iodine at these sites. Significant increases in $^{129}I/I$ ratios uphole are found just above the lithologic boundary between the overlying forearc basin and older accreted sediments. This observation suggests that only limited migration of ascending deep fluids occurs beyond the lithologic boundary, where sediment porosity drops abruptly from 60% to 50%, and that fluids move preferentially along the lithologic boundary.

Introduction

Integrated Ocean Drilling Program (IODP) Expeditions 315 and 316 were carried out in 2007 and 2008 by the D/V *Chikyu* as part of the multistage Nankai Trough Seismogenic Zone Experiment (NanTroSEIZE) complex drilling project. During these expeditions, Kumano forearc basin sediment was cored to the upper accretionary prism as well as into the accretionary prism itself, including a fractured/brecciated zone associated with subduction processes in the Nankai Trough, Japan. Interstitial fluid collected from these sediments preserve a complex history of fluid-rock interaction and migration through the aquifer and the entire sediment body. Application of the iodine radioisotope (^{129}I) system has been useful to extract geochronological signatures from interstitial fluid geochemistry (Fehn et al., 2000). In this research, we focus on iodine concentrations and $^{129}I/I$ ratios in the interstitial fluid regime, covering the lithologic boundary between different sedimentary systems.

doi:10.2204/iodp.proc.314315316.220.2012

Geological settings

During Expedition 315, the upper accretionary prism was cored at two sites: IODP Site C0001 at the seaward edge of the Kumano Basin uplift (outer arc high) and IODP Site C0002 at the southern margin of the basin. Holocene to late Pliocene silty clay to clayey silt is unconformably underlain by the late Miocene upper accretionary prism composed mainly of mudstone and bounded by a thick sand layer at 207 m core depth below seafloor (CSF) at Site C0001 (Ashi et al., 2008; Kinoshita et al., 2008). An unconformity between the forearc basin and accretionary prism is identified by the lithology change from basal Pliocene mudstone above to late Miocene interbeds of mudstone and sandstone below at 922 m CSF at Site C0002 (Ashi et al., 2008). During Expedition 316, the seaward edge of the Kumano Basin uplift where the megasplay fault is branching from the plate interface between the subducting Philippine Sea plate and overlying Eurasian plate was cored at IODP Site C0004. A 6 cm thick microbreccia, indicating concentrated shear within the megasplay fault zone, was found in the middle Pliocene hemipelagic section at 291 m CSF. IODP Site C0008 is located ~1 km seaward of Site C0004, providing a reference site for the sediments underthrusting beneath the megasplay fault (Kimura et al., 2008).

Iodine geochronology in marine environments

Iodine concentrations in marine interstitial fluid from continental margins have been reported to rapidly increase with depth (Martin et al., 1993; Fehn et al., 1992; Tomaru et al., 2007b, 2009). This increase is ascribed to the strongest association of iodine with organic matter; sedimentation and subsequent degradation of iodine-rich organic matter at depth liberates iodine into the interstitial fluid, resulting in iodine concentrations considerably higher than typical seawater levels of 0.4 µM (Broecker and Peng, 1982; Burton, 1996; Muramatsu and Wedepohl, 1998).

The presence of the long-lived cosmogenic radioisotope ^{129}I ($T_{1/2}$ = 15.7 m.y.) has been used to date the time of separation of organic matter from the marine system (Fabryka-Martin et al., 1987; Fehn et al., 2000). The initial ratio for dating of iodine in the marine environment has been determined to be $(1500 \pm 150) \times 10^{-15}$, which results in a dating range of ~80 m.y. for the ^{129}I isotopic system (Fehn et al., 2007). The ^{129}I/I ratio of interstitial fluid is sometimes modified by the input of fissiogenic ^{129}I, which is produced by the spontaneous fission of ^{238}U and released into interstitial fluid during migration through the sediment column. In the case here, however, fissiogenic input is negligible because of relatively low U concentration of 0.99 ppm in the subducting sediments in the Nankai Trough and high interstitial fluid iodine concentration (Fabryka-Martin et al., 1989; Plank and Langmuir, 1998; Tomaru et al., 2007a). Standard decay of ^{129}I thus provides the elapsed time since the organic matter enriched in iodine has been isolated from seawater as (Fehn et al., 2007)

$$R_{obs} = R_i e^{-\lambda_{129} t}, \quad (1)$$

where

R_{obs} = observed ^{129}I/I ratio,
R_i = initial seawater ^{129}I/I ratio of 1500×10^{-15},
λ_{129} = decay constant of ^{129}I (4.41×10^{-8} y^{-1}), and
t = years since iodine deposition.

Although fissiogenic ^{129}I or anthropogenic ^{129}I are unlikely to have contributed to interstitial fluid in locations like those studied here (e.g., Fehn et al., 2000; Tomaru et al., 2007a), contribution from either source would have raised the ratio. The values calculated for the samples here are therefore minimum ages.

Analytical methods

A 20–50 cm long whole-round core was sectioned soon after core recovery and scraped in a nitrogen-filled glove bag to avoid surface sediments that could have been contaminated with seawater, drilling fluid, oxidation, and/or smearing in the borehole. The core section was then squeezed with a shipboard hydraulic press to extract interstitial fluid through 0.45 µm filters. A sample aliquot was diluted with 5% tetramethyl ammonium hydroxide (TMAH) solution for the determination of total dissolved iodine concentration and measured by inductively coupled plasma–mass spectrometer (ICP-MS), HP4500 (Hewlett Packard/Agilent), at the University of Tokyo, with a standard deviation better than 2.7%. All concentrations are listed in Table **T1** together with depth.

For the measurement of ^{129}I/I ratio, silver iodide (AgI) was precipitated from the interstitial fluid samples by extracting iodine reduced from iodate with sodium bisulfite into chloroform (Fehn et al., 1992; Lu et al., 2010). Because >0.1 mg of AgI is required for reliable ^{129}I/I analyses (Lu et al., 2007), we combined 3–7 neighboring samples from Sites C0001 and C0002. These targets were analyzed for ^{129}I/I ra-

tios at PRIME Lab, Purdue University (Sharma et al., 2000). The weighted average depth and iodine concentration of $^{129}I/I$ samples are calculated from iodine concentrations and volume of sample aliquots combined for AgI precipitation (Table T2). Error margins for depth in the $^{129}I/I$ profile therefore reflect the interval between the shallowest and deepest aliquots.

Results

Iodine concentrations dissolved in interstitial fluid generally increase rapidly in the uppermost 100 m CSF and thereafter reach relatively constant values at ~200 µM at all sites (Fig. F1). The most pronounced increase is observed at Site C0002, where iodine concentrations reach values >400 µM but decrease to values comparable to the other sites at greater depths. Consistent with earlier results from the Nankai Trough area, interstitial fluid iodine concentrations here are exceedingly higher than that of seawater (0.4 µM), which has been interpreted as evidence for the input of deep fluids receiving iodine from degradation of marine organic matter (You et al., 1993; Fehn et al., 2003; Muramatsu et al., 2007; Tomaru et al., 2007a). Linear iodine profiles starting at ~200 m CSF at Site C0001, above 477 m CSF at Site C0002, ~150 m CSF at Site C0004, and ~100 m CSF at Site C0008 indicate that iodine from organic matter decomposed in deeper sediments dominates in these intervals and mixes with iodine from seawater in the shallower sections. There is probably only minor iodine input from host sediments because iodine concentrations in sediment and interstitial fluid do not show apparent covariation within this depth window in the Nankai Trough (Muramatsu et al., 2007).

The interstitial fluid $^{129}I/I$ ratios at Site C0001 gradually decrease downhole from 938 × 10^{-15} at 41 m CSF to ~400 × 10^{-15} at ~200 m CSF, providing minimum iodine ages from 10.6 to ~30 Ma (Equation 1), where the lithologic boundary between the old accretionary prism and overlying younger forearc basin sediment is located (Fig. F2). This gradient represents mixing of iodine between deep fluids ($^{129}I/I$ = 400 × 10^{-15}) and young iodine mainly from seawater ($^{129}I/I$ = 1500 × 10^{-15}) because iodine concentrations in this interval are modulated by seawater input (Fig. F1). On the other hand, iodine ages at adjoining Site C0002 are relatively constant at ~30 Ma throughout the sediment column (Fig. F2), deep old iodine is dominant even in the interval just below the seafloor with relatively low iodine concentrations.

The results suggest that iodine in interstitial fluid is significantly older than the host sediment because young iodine inputs that potentially increase $^{129}I/I$ ratios (decrease iodine age) are minor according to the depth profile of iodine concentrations. Significant inputs of young iodine probably from seawater are observed only in the shallow section at Site C0001. A similar co-existence of iodine with organic matter was observed in fluid from Ocean Drilling Program Leg 131 in the toe of the Nankai Trough accretionary prism, ~190 km southwest of these sites, pointing to fluid advection along the décollement zone from organic matter–rich sediments further in the accretionary prism (You et al., 1993). This observation agrees well with the occurrence of fluids much older than the host sediments at Sites C0001 and C0002.

Concerning $^{129}I/I$ variation, the old iodine flux from old accreted sediments reaches the overlying young basin sediments at Site C0002; however, old iodine dominates only in the old accretionary prism and younger iodine plays a more important role in the younger basin sediments at Site C0001. This difference probably reflects changes of fluid modes between locations, which correlates well with changes in sediment porosity, a fundamental geophysical factor controlling fluid transport (Screaton et al., 2002; Ashi et al., 2008; Kinoshita et al., 2008). A discontinuous porosity change is found at the lithologic boundary only at Site C0001, where porosity changes from ~50% above the boundary to ~60% below (Fig. F2). Because the upward fluid transport can be interrupted by the porosity drop of ~10%, fluids are more likely at this location to escape along the boundary rather than cross it. As shown in the porosity distribution, more compacted and deeper sediments at Site C0002 probably form a more uniform lithologic boundary for fluid migration than at Site C0001.

Acknowledgments

This research used samples and data provided by the Integrated Ocean Drilling Program from Expeditions 315 and 316. We thank the crew and technical staff of the *Chikyu* for making this expedition a success. We are grateful for $^{129}I/I$ determinations at PRIME Lab, Purdue University. This study was supported by the Japan Agency for Marine-Earth Science and Technology, the National Science Foundation, and the Research Fellowships of the Japan Society for the Promotion of Science for Young Scientists.

References

Ashi, J., Lallemant, S., Masago, H., and the Expedition 315 Scientists, 2008. NanTroSEIZE Stage 1A: NanTroSEIZE

megasplay riser pilot. *IODP Prel. Rept.,* 315. doi:10.2204/iodp.pr.315.2008

Broecker, W.S., and Peng, T.-H., 1982. *Tracers in the Sea:* Palisades, NY (Eldigio Press).

Burton, J.D., 1996. The ocean: a global geochemical system. *In* Summerhayes, C.P., and Thorpe, S.A. (Eds.), *Oceanography: An Illustrated Guide:* London (Manson Publishing Ltd.), 165–181.

Fabryka-Martin, J., Davis, S.N., and Elmore, D., 1987. Applications of ^{129}I and ^{36}Cl in hydrology. *Nucl. Instrum. Methods Phys. Res., Sect. B,* 29(1–2):361–371. doi:10.1016/0168-583X(87)90265-5

Fabryka-Martin, J.T., Davis, S.N., Elmore, D., and Kubik, P.W., 1989. In situ production and migration of ^{129}I in the Stripa granite, Sweden. *Geochim. Cosmochim. Acta,* 53(8):1817–1823. doi:10.1016/0016-7037(89)90302-5

Fehn, U., Moran, J.E., Snyder, G.T., and Muramatsu, Y., 2007. The initial ^{129}I/I ratio and the presence of "old" iodine in continental margins. *Nucl. Instrum. Methods Phys. Res., Sect. B,* 259(1):496–502. doi:10.1016/j.nimb.2007.01.191

Fehn, U., Peters, E.K., Tullai-Fitzpatrick, S., Kubik, P.W., Sharma, P., Teng, R.T.D., Gove, H.E., and Elmore, D., 1992. ^{129}I and ^{36}Cl concentrations in waters of the eastern Clear Lake area, California: residence times and source ages of hydrothermal fluids. *Geochim. Cosmochim. Acta,* 56(5):2069–2079. doi:10.1016/0016-7037(92)90330-L

Fehn, U., Snyder, G., and Egeberg, P.K., 2000. Dating of pore waters with ^{129}I: relevance for the origin of marine gas hydrates. *Science,* 289(5488):2332–2335. doi:10.1126/science.289.5488.2332

Fehn, U., Snyder, G.T., Matsumoto, R., Muramatsu, Y., and Tomaru, H., 2003. Iodine dating of pore waters associated with gas hydrates in the Nankai area, Japan. *Geology,* 31(6):521–524. doi:10.1130/0091-7613(2003)031<0521:IDOPWA>2.0.CO;2

Kimura, G., Screaton, E.J., Curewitz, D., and the Expedition 316 Scientists, 2008. NanTroSEIZE Stage 1A: NanTroSEIZE shallow megasplay and frontal thrusts. *IODP Prel. Rept.,* 316. doi:10.2204/iodp.pr.316.2008

Kinoshita, M., Tobin, H., Moe, K.T., and the Expedition 314 Scientists, 2008. NanTroSEIZE Stage 1A: NanTroSEIZE LWD transect. *IODP Prel. Rept.,* 314. doi:10.2204/iodp.pr.314.2008

Lu, Z., Fehn, U., Tomaru, H., Elmore, D., and Ma, X., 2007. Reliability of ^{129}I/I ratios produced from small sample masses. *Nucl. Instrum. Methods Phys. Res., Sect. B,* 259(1):359–364. doi:10.1016/j.nimb.2007.01.180

Lu, Z., Fehn, U., Zhao, X., Kieser, W.E., and Tomaru, H., 2010. Comparison of three chemical extraction methods for I-129 determinations. *Nucl. Instrum. Methods Phys. Res., Sect. B,* 268(7–8):952–955. doi:10.1016/j.nimb.2009.10.072

Martin, J.B., Gieskes, J.M., Torres, M., and Kastner, M., 1993. Bromide and iodine in Peru margin sediments and pore fluids: implications for fluid origins. *Geochim. Cosmochim. Acta,* 57(18):4377–4389. doi:10.1016/0016-7037(93)90489-J

Muramatsu, Y., Doi, T., Tomaru, H., Fehn, U., Takeuchi, R., and Matsumoto, R., 2007. Halogen concentrations in pore waters and sediments of the Nankai Trough, Japan: implications for the origin of gas hydrates. *Appl. Geochem.,* 22(3):534–556. doi:10.1016/j.apgeochem.2006.12.015

Muramatsu, Y., and Wedepohl, K.H., 1998. The distribution of iodine in the Earth's crust. *Chem. Geol.,* 147(3–4):201–216. doi:10.1016/S0009-2541(98)00013-8

Plank, T., and Langmuir, C.H., 1998. The chemical composition of subducting sediment and its consequences for the crust and mantle. *Chem. Geol.,* 145(3–4):325–394. doi:10.1016/S0009-2541(97)00150-2

Screaton, E., Saffer, D., Henry, P., and Hunze, S., 2002. Porosity loss within the underthrust sediments of the Nankai accretionary complex: implications for overpressures. *Geology,* 30(1):19–22. doi:10.1130/0091-7613(2002)030<0019:PLWTUS>2.0.CO;2

Sharma, P., Bourgeois, M., Elmore, D., Lipschutz, M.E., Ma, X., Miller, T., Mueller, K., Rickey, K., Simms, P., and Vogt, S., 2000. PRIME Lab AMS performance, upgrades, and research applications. *Nucl. Instrum. Methods Phys. Res., Sect. B,* 172(1–4):112–123. doi:10.1016/S0168-583X(00)00132-4

Tomaru, H., Fehn, U., Lu, Z., Takeuchi, R., Inagaki, F., Imachi, H., Kotani, R., Matsumoto, R., and Aoike, K., 2009. Dating of dissolved iodine in pore waters from the gas hydrate occurrence offshore Shimokita Peninsula, Japan: ^{129}I results from D/V *Chikyu* shakedown cruise. *Resour. Geol.,* 59(4):359–373. doi:10.1111/j.1751-3928.2009.00103.x

Tomaru, H., Lu, Z., Fehn, U., Muramatsu, Y., and Matsumoto, R., 2007a. Age variation of pore water iodine in the eastern Nankai Trough, Japan: evidence for different methane sources in a large gas hydrate field. *Geology,* 35(11):1015–1018. doi:10.1130/G24198A.1

Tomaru, H., Lu, Z., Snyder, G.T., Fehn, U., Hiruta, A., and Matsumoto, R., 2007b. Origin and age of pore waters in an actively venting gas hydrate field near Sado Island, Japan Sea: interpretation of halogen and ^{129}I distributions. *Chem. Geol.,* 236(3–4):350–366. doi:10.1016/j.chemgeo.2006.10.008

You, C.-F., Gieskes, J.M., Chen, R.F., Spivack, A., and Gamo, T., 1993. Iodide, bromide, manganese, boron, and dissolved organic carbon in interstitial waters of the organic carbon–rich marine sediments: observations in the Nankai accretionary prism. *In* Hill, I.A., Taira, A., Firth, J.V., et al., *Proc. ODP, Sci. Results,* 131: College Station, TX (Ocean Drilling Program), 165–174. doi:10.2973/odp.proc.sr.131.116.1993

Initial receipt: 4 August 2011
Acceptance: 26 October 2011
Publication: 9 January 2012
MS 314315316-220

Figure F1. Depth profiles of iodine concentrations. No samples were recovered at Site C0002 between 201 and 477 m CSF. Red and blue dashed lines = lithologic boundary between overlying Kumano forearc basin sediment and underlying accreted sediments at Sites C0001 and C0002, respectively (Ashi et al., 2008), green band = brecciated/fractured zone of megasplay fault (Kimura et al., 2008), arrows = iodine seawater value of 0.4 µM (Broecker and Peng, 1982; Burton, 1996).

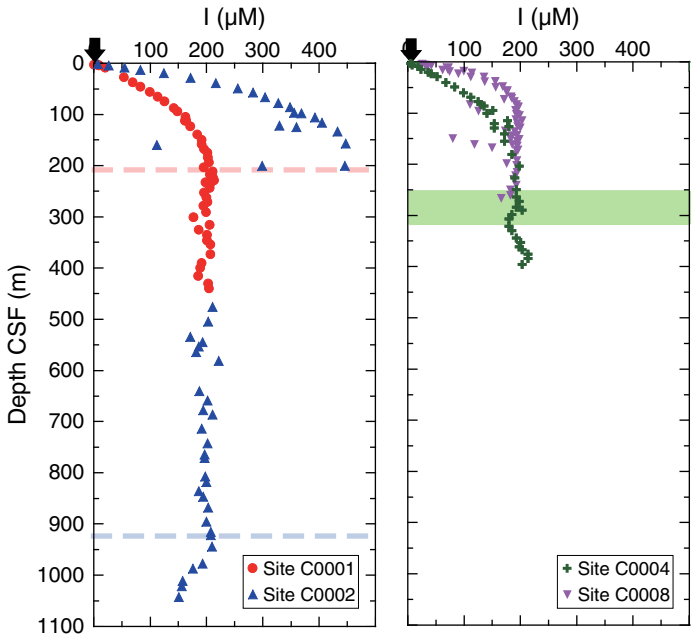

Figure F2. Depth profiles of $^{129}I/I$ ratio and sediment porosity obtained from logging while drilling (Kinoshita et al., 2008). Red and blue dashed lines = lithologic boundary between overlying Kumano forearc basin sediment and underlying accreted sediments at Sites C0001 and C0002, respectively (Ashi et al., 2008), arrow = seawater value for $^{129}I/I$ of 1500×10^{-15} (Fehn et al., 2007). Ages are calculated from the measured $^{129}I/I$ ratio with the standard decay equation of ^{129}I (Equation 1).

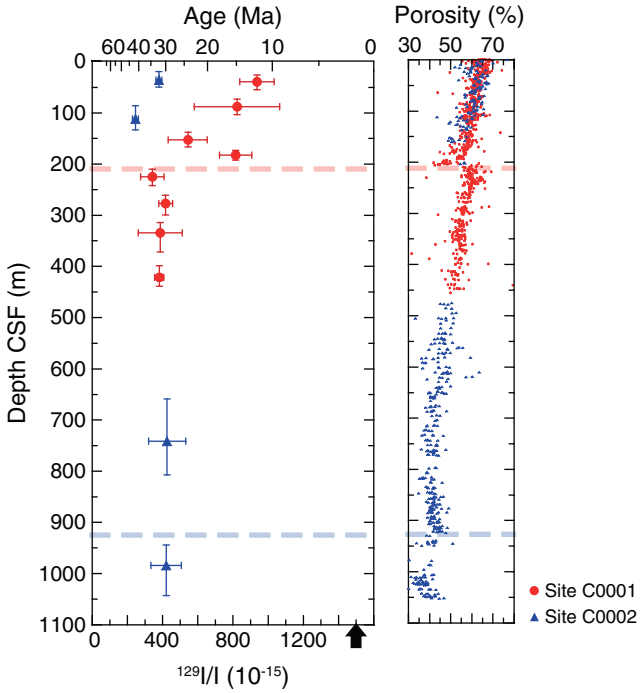

Table T1. Analytical results of iodine concentration in interstitial fluid from IODP Expeditions 315 and 316. (Continued on next page.)

Core, section	Depth CSF (m)	Iodine (μM)
315-C0001E-		
1H-4	3.00	0.983
1H-6	3.91	8.68
1H-7	4.14	9.21
2H-4	8.74	20.6
4H-4	27.52	53.2
5H-4	37.03	69.1
6H-4	46.23	82.8
7H-4	55.83	99.6
8H-4	65.22	113
9H-4	74.89	126
10H-7	87.27	142
11H-4	93.71	149
12H-5	104.62	163
13H-4	112.77	162
315-C0001F-		
1H-4	112.11	164
2H-5	123.04	171
4H-3	139.20	184
5H-4	149.98	191
6H-4	158.55	192
7H-12	168.04	196
8H-4	175.11	202
9H-4	184.00	203
10H-10	193.35	205
13H-2	203.23	196
14H-4	211.32	211
15H-4	217.30	207
18H-4	222.72	212
19H-4	228.34	214
20X-5	235.34	207
21X-4	243.42	206
315-C0001H-		
1R-3	232.63	199
3R-4	253.02	196
4R-4	262.54	200
5R-3	270.64	202
6R-2	278.71	195
7R-4	291.06	200
8R-4	300.93	177
10R-4	316.06	206
11R-4	325.55	186
12R-4	335.06	201
13R-5	345.95	201
14R-4	354.04	207
16R-4	373.04	207
18R-3	390.64	192
19R-3	400.12	189
21R-3	415.12	186
23R-2	430.57	203
24R-2	440.14	205
315-C0002B-		
1R-2	476.58	211
4R-2	504.76	203
8R-2	534.57	171
9R-3	545.15	193
10R-2	553.56	186
11R-3	564.47	182
13R-2	582.07	222
19R-3	640.52	188
21R-3	659.10	202
23R-3	678.03	194
24R-2	686.12	211
27R-2	714.27	192
30R-2	743.07	202
32R-5	764.50	197
33R-2	771.20	197
37R-2	807.12	198
38R-3	818.03	200
40R-2	835.62	186
41R-3	846.53	194
43R-5	867.95	203
46R-4	895.01	200
48R-5	915.45	208
49R-3	922.11	208
51R-5	943.91	210
55R-2	977.70	193
56R-2	986.85	176
59R-2	1011.12	158
61R-3	1021.53	156
64R-2	1043.20	151
315-C0002D-		
1H-2	1.52	7.15
1H-5	4.35	26.8
2H-3	8.81	54.9
2H-7	13.06	82.9
3H-4	19.54	124
4H-4	29.20	172
5H-4	38.71	217
6H-5	49.43	256
7H-4	57.74	283
8H-4	66.92	304
9H-5	78.10	328
10H-4	86.21	348
11H-5	96.72	355
11H-6 (HYD)	98.06	369
12H-5	106.41	393
13H-5	115.81	405
14H-3 (HYD)	121.92	330
14H-5	124.74	360
15X-5	133.18	433
16H-6	157.09	448
17X-4 (HYD)	159.77	112
18H-1 (HYD)	200.42	299
18H-2	200.60	446
315-C0004C-		
1H-3	2.73	3.81
1H-6	5.54	7.54
2H-3	9.09	16.9
2H-7	13.38	24.1
3H-5	20.01	35.7
3H-8	22.87	42.2
4H-4	29.52	52
5H-4	39.17	68.5
6H-4	48.58	83.4
7H-6	59.45	98.2
8H-4	67.74	111
9H-4	77.25	125
10H-3	83.58	131
11H-2	86.35	136
12X-6	95.12	150
13X-3	101.40	139
14X-5	113.72	176
15X-7	126.05	180
315-C0004D-		
3R-2	119.99	153
4R-2	129.17	154
5R-3	139.69	171
7R-2	153.08	172
13R-2	179.47	186
16R-2	203.20	197
19R-2	226.82	190

Table T1 (continued).

Core, section	Depth CSF (m)	Iodine (μM)
23R-1	248.12	193
26R-3	262.69	193
28R-2	271.91	197
30R-3	282.19	193
32R-3	290.21	202
34R-1	296.75	185
36R-2	306.80	181
39R-2	320.29	180
41R-2	329.45	186
44R-3	344.20	193
46R-2	352.06	201
48R-2	361.16	197
49R-2	365.81	202
51R-2	375.63	213
53R-2	384.10	212
55R-2	393.60	204
316-C0008A-		
1H-3	1.75	1.42
1H-7	5.54	24.1
2H-2	8.46	34.2
2H-8	15.55	61.9
3H-3	18.52	74.5
3H-8	23.10	90.2
4H-4	29.30	112
5H-4	38.83	137
6H-5	49.38	156
7H-5	58.73	176
8H-5	68.37	184
9H-5	77.70	190
10H-6	87.37	196
11H-4	94.87	193
12H-5	105.05	199
13H-5	114.93	203
15H-2	120.31	195
16H-4	128.96	200
17H-6	136.28	190
18H-3	143.15	194
19H-2	151.52	198
20H-3	155.24	194
21H-5	164.26	195
22H-6	173.76	194
23H-5	182.18	190
24H-6	192.93	194
25H-2	198.36	176
26H-2	202.37	193
27H-5	215.79	194
28H-3	222.37	191
29X-5	229.41	188
30X-7	240.34	193
31X-6	250.11	182
32X-7	260.91	182
33X-4	266.86	166
316-C0008B-		
1H-5	5.77	31.5
316-C0008C-		
1H-2	1.55	1.07
1H-5	4.38	25.9
2H-2	6.94	41.5
2H-7	12.31	70.9
3H-3	17.85	99.6
3H-7	22.05	114
4H-5	29.50	135
5H-5	38.13	156
6H-4	47.88	169
7H-4	55.99	177
9H-4	70.82	185
9H-7	73.14	172
10H-9	83.41	194
10H-12	85.51	128
11H-2	82.91	110
11H-10	88.22	197
13H-8	94.99	191
13H-10	95.98	126
14H-6	102.82	193
15H-5	103.44	194
16H-5	112.46	192
18H-6	126.36	195
21H-5	134.55	174
22X-5	144.22	186
23X-2	149.75	80
23X-4	150.51	183
24X-4	161.17	186
24X-5	161.43	119
25X-2	167.41	150
25X-9	171.76	196

Table T2. Analytical results of $^{129}I/I$ ratio of interstitial fluid from IODP Expedition 315.

Hole	Average depth CSF (m)*	Average I (μM)*	$^{129}I/I$ (10^{-15})†	Age (Ma)
315-				
C0001E	41.0	71.91	938 ± 98.1	10.6
C0001E	89.6	143.2	825 ± 243	13.6
C0001F	154.3	190.8	545 ± 110	22.9
C0001F	183.9	203.1	817 ± 92.7	13.8
C0001F	226.2	209.2	344 ± 66.9	33.3
C0001F	278.9	196.7	420 ± 40.3	28.9
C0001F	336.1	202.4	388 ± 124	30.6
C0001F	423.0	195.6	383 ± 26.0	31.0
C0002B	741.3	197.3	426 ± 105	28.5
C0002B	984.2	180.8	421 ± 86.3	28.8
C0002D	36.3	187.4	379 ± 16.4	31.2
C0002D	111.9	400.1	246 ± 16.1	41.0

* = weighted average depth and concentration were calculated from iodine concentration and volume of sample aliquots combined in the sample for $^{129}I/I$ measurement. † = iodine age is calculated from standard decay equation of ^{129}I with an initial $^{129}I/I$ ratio of 1500×10^{-15}.